LETTER

doi:10.1038/nature09973

TLR signalling augments macrophage bactericidal activity through mitochondrial ROS

A. Phillip West[1], Igor E. Brodsky[1]†, Christoph Rahner[2], Dong Kyun Woo[3], Hediye Erdjument-Bromage[4], Paul Tempst[4], Matthew C. Walsh[5], Yongwon Choi[5], Gerald S. Shadel[3] & Sankar Ghosh[6]

Reactive oxygen species (ROS) are essential components of the innate immune response against intracellular bacteria and it is thought that professional phagocytes generate ROS primarily via the phagosomal NADPH oxidase machinery[1]. However, recent studies have suggested that mitochondrial ROS (mROS) also contribute to mouse macrophage bactericidal activity, although the mechanisms linking innate immune signalling to mitochondria for mROS generation remain unclear[2–4]. Here we demonstrate that engagement of a subset of Toll-like receptors (TLR1, TLR2 and TLR4) results in the recruitment of mitochondria to macrophage phagosomes and augments mROS production. This response involves translocation of a TLR signalling adaptor, tumour necrosis factor receptor-associated factor 6 (TRAF6), to mitochondria, where it engages the protein ECSIT (evolutionarily conserved signalling intermediate in Toll pathways), which is implicated in mitochondrial respiratory chain assembly[5]. Interaction with TRAF6 leads to ECSIT ubiquitination and enrichment at the mitochondrial periphery, resulting in increased mitochondrial and cellular ROS generation. ECSIT- and TRAF6-depleted macrophages have decreased levels of TLR-induced ROS and are significantly impaired in their ability to kill intracellular bacteria. Additionally, reducing macrophage mROS levels by expressing catalase in mitochondria results in defective bacterial killing, confirming the role of mROS in bactericidal activity. These results reveal a novel pathway linking innate immune signalling to mitochondria, implicate mROS as an important component of antibacterial responses and further establish mitochondria as hubs for innate immune signalling.

The phagocytic response of the innate immune system involves the production of ROS via the phagosomal NADPH-oxidase-dependent respiratory burst. This is a necessary effector response for the destruction of intracellular microbes[1,6]. In addition to NADPH-oxidase, the mitochondrial oxidative phosphorylation machinery generates ROS when electrons prematurely escape oxidative phosphorylation complexes I and III and react with molecular oxygen to generate superoxide[7,8]. Mitochondria are major sites of ROS production in most cells; however, mROS have traditionally been regarded as byproducts of oxidative respiration and therefore their synthesis was believed to be unregulated[7,9]. To examine whether TLR signalling could enhance mROS production we stimulated RAW 264.7 macrophages (RAW cells) with lipopolysaccharide (LPS, a TLR4 agonist), synthetic lipopeptide Pam3CSK4 (TLR1 and TLR2 agonist), lipotechoic acid (LTA, TLR2 agonist), poly(I:C) (TLR3 agonist), R848 (TLR7 and TLR8 agonist) and CpG DNA (TLR9 agonist) (Fig. 1a). The production of mROS was triggered only upon signalling from the cell-surface TLRs (TLR1, TLR2 and TLR4), whereas stimulation of endosomal TLRs (TLR3, TLR7, TLR8 and TLR9) failed to augment mROS (Fig. 1a). Exposure of cells to rotenone and antimycin A, compounds known to increase mitochondrial superoxide generation, did augment mROS but treatment with tumour-necrosis factor-α (TNF-α) did not (Fig. 1a)[7]. We observed similar increases in mROS when bone-marrow-derived macrophages (BMDMs) were stimulated with TLR1, TLR2 and TLR4 (TLR1/2/4) agonists but we were again unable to detect significant induction of mROS upon ligation of TLR9 (Fig. 1b). We also detected increased cellular hydrogen peroxide (H_2O_2) generation upon TLR2/TLR4 ligation, but not after TLR9 ligation (Fig. 1b)[10–12]. As ROS are critical for antibacterial responses,

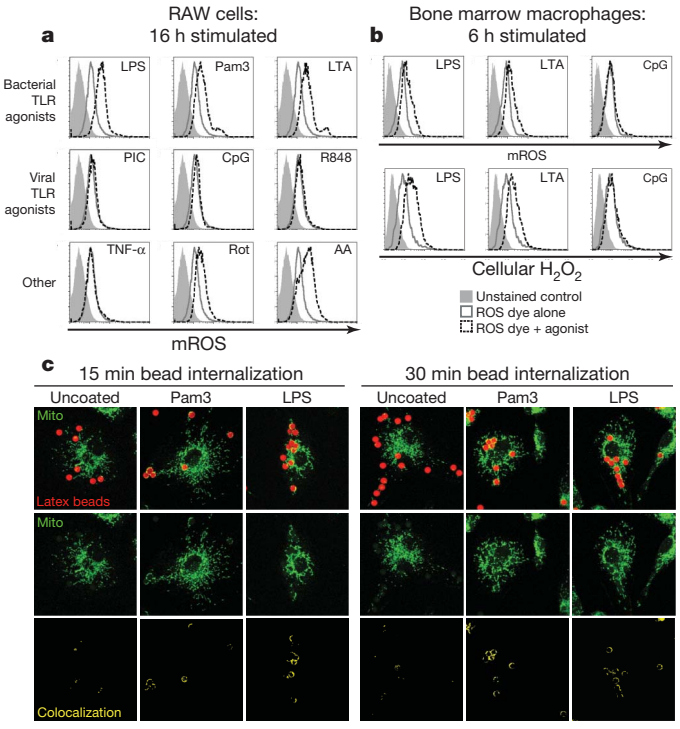

Figure 1 | TLR1/2/4 signalling induces mROS generation and mitochondrial recruitment to phagosomes. a, RAW cells stimulated as indicated, stained with MitoSOX (mROS) and analysed by fluorescence-activated cell sorting (FACS). Pam3, Pam3CSK4; PIC, poly(I:C); Rot, rotenone; AA, antimycin A. **b**, BMDMs stimulated as indicated, stained with MitoSOX (top panels) or CM-H_2DCFDA (cellular H_2O_2, bottom panels) and analysed by FACS. **c**, BMDMs were incubated with uncoated, Pam3CSK4-coated or LPS-coated latex beads, mitochondrial networks were immunostained with HSP70 antibodies (Mito) and confocal Z-stacks were acquired. Co-localized beads (red pixels) and mitochondria (green pixels) are displayed in yellow (bottom). Images shown are representative of approximately 100 cells analysed at ×63 original magnification.

[1]Department of Immunobiology, Yale University School of Medicine, New Haven, Connecticut 06520, USA. [2]Department of Cell Biology, Yale University School of Medicine, New Haven, Connecticut 06520, USA. [3]Department of Pathology, Yale University School of Medicine, New Haven, Connecticut 06520, USA. [4]Molecular Biology Program, Memorial Sloan-Kettering Cancer Center, New York, New York 10021, USA. [5]Department of Pathology and Laboratory Medicine, University of Pennsylvania School of Medicine, Philadelphia, Pennsylvania 19104, USA. [6]Department of Microbiology and Immunology, College of Physicians and Surgeons, Columbia University, New York, New York 10032, USA. †Present address: Department of Pathobiology, University of Pennsylvania School of Veterinary Medicine, Philadelphia, Pennsylvania 19104, USA.

it is not surprising that signalling from cell-surface TLRs, which predominantly recognize ligands derived from bacteria, induces ROS generation[13]. In contrast, ROS are not used as direct antiviral effectors and hence endosomal TLRs, which function primarily in sensing viral infection, do not seem to augment ROS production.

Several reports have indicated that mitochondria are recruited to vacuoles containing intracellular pathogens[14–17]. To investigate whether recruitment of mitochondria to phagosomes might be an active process mediated by innate immune signalling, we examined mitochondrial localization in cells loaded with latex beads coated with pathogen-associated molecular patterns (PAMPs). Such coated beads have been used previously to investigate signalling in phagocytic cells and have been shown to recruit innate immune signalling components, analogous to phagocytosed bacteria[18,19]. Interestingly, we observed mitochondrial recruitment and cupping around Pam3CSK4- and LPS-coated beads in BMDMs (Fig. 1c). Uncoated beads, despite being taken up by BMDMs to a similar extent, did not co-localize efficiently with mitochondrial networks and displayed markedly lower mitochondrial cupping per bead (Fig. 1c and Supplementary Fig. 2).

On the basis of the above findings, we hypothesized that the inducible juxtaposition of phagosomes and mitochondria should be accompanied by the concomitant translocation of TLR signalling components. A key intermediate in TLR1/2/4 signalling is TRAF6 and immunoblotting of highly purified cellular extracts from LPS-stimulated macrophages revealed that TRAF6 was enriched in mitochondrial fractions (Fig. 2a). This recruitment was specific to TRAF6 because other cytosolic proteins that interact transiently with TLR signalling complexes, such as MyD88, IRAK4 (not shown), IRAK1, TAK1, and IκBα, were not detected in mitochondrial fractions. Furthermore, stimulation with Pam3CSK4 and LTA induced TRAF6 recruitment to mitochondria with similar kinetics to that triggered by LPS (Fig. 2b). Consistent with the results concerning mROS generation, we were unable to detect TRAF6 in the mitochondrial fractions of macrophages stimulated with poly(I:C) or CpG (Fig. 2c).

The induction of mROS and the recruitment of TRAF6 to mitochondria upon TLR1/2/4 stimulation indicated that TRAF6 might interact with mitochondrial proteins to control mROS production. Recent studies have shown that ECSIT, a previously characterized TRAF6-interacting protein, localizes to mitochondria and has a role in oxidative phosphorylation complex I assembly[5,20,21]. Mass spectrometry analysis of purified ECSIT protein complexes confirmed that ECSIT associates with oxidative phosphorylation complex I components (Supplementary Table 1). Immunofluorescence microscopy and biochemical fractionation experiments revealed that ECSIT localizes predominantly to mitochondria in both fibroblasts and BMDMs (Supplementary Fig. 3a–c). Additional analysis confirmed that ECSIT localizes to the inner mitochondrial membrane, consistent with its role in complex I assembly[5]. However, we also observed some ECSIT molecules proximal to outer mitochondrial membranes (OMMs), indicating that OMM-associated ECSIT might interact with TRAF6 recruited from phagosomal TLR signalling complexes (Supplementary Fig. 3d–f). Accordingly, we detected inducible interactions between ECSIT and TRAF6 in purified mitochondrial extracts from macrophages stimulated with LPS (Fig. 2d).

TRAF6 possesses E3-ubiquitin ligase activity; therefore, we explored whether ECSIT is ubiquitinated by TRAF6 (ref 22, 23). ECSIT was polyubiquitinated when co-transfected with TRAF6 in HEK 293 cells (Supplementary Fig. 4a) and a dominant-negative form of ECSIT lacking the TRAF6 interaction domain was significantly less ubiquitinated by TRAF6 than wild-type ECSIT (Supplementary Fig. 4b)[21]. We also detected an increase in ECSIT polyubiquitination in macrophages after exposure to LPS, which mirrored the mitochondrial recruitment kinetics of TRAF6 (Supplementary Fig. 4c). In addition, total LPS-induced ECSIT ubiquitination was decreased in TRAF6-knockdown macrophages, indicating a requirement for TRAF6 in the ubiquitination of ECSIT during TLR4 signalling (Supplementary Fig. 4c).

We next investigated the dynamics of ECSIT localization in mitochondria after LPS stimulation. Notably, after 30 min of LPS treatment, ECSIT became more sensitive to proteinase K in the absence of OMM permeabilization by saponin (Fig. 2e). In contrast, the inner mitochondrial membrane protein NDUFS3 remained largely insensitive to proteinase K without saponin treatment. This indicates that ECSIT becomes enriched at the mitochondrial periphery, and thus becomes more sensitive to protease digestion, upon LPS signalling. Electron microscopy analysis further confirmed these data, as more ECSIT was localized peripheral to the OMM after LPS treatment (Supplementary Fig. 5). Protease sensitivity assays on mitochondria from TRAF6-knockdown RAW cells indicated that TRAF6 is required for LPS-induced ECSIT enrichment on OMMs (Supplementary Fig. 6, compare lanes 5 and 7 with 9 and 11). In addition to influencing the mitochondrial localization of ECSIT, TRAF6–ECSIT signalling also appears to regulate the recruitment of mitochondria around PAMP-coated latex beads. Both TRAF6-knockout and ECSIT-knockdown BMDMs showed less mitochondrial enrichment around phagosomes containing LPS- and Pam3CSK4-coated beads than did wild-type BMDMs (Supplementary Fig. 7).

The link between ECSIT and complex I led us to hypothesize that ECSIT might modulate mROS derived from this complex[5,7]. To

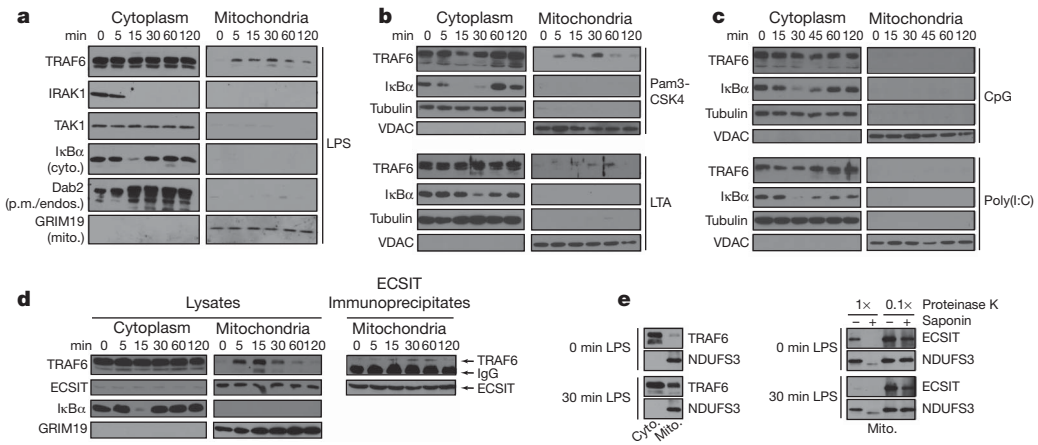

Figure 2 | TRAF6 is recruited to mitochondria upon TLR1/2/4, but not TLR3/9, signalling to engage ECSIT on the mitochondrial surface. **a–e**, RAW cells were stimulated with TLR agonists for the indicated times, cells were fractionated and extracts were western-blotted. cyt., cytoplasmic localization; p.m./endos., plasma membrane/endosomes localization; mito., mitochondrial localization. **d**, Purified mitochondrial lysates were immunoprecipitated with ECSIT antibody overnight. **e**, Equal amounts of extracts were treated with the indicated amount of proteinase K (1×, 33 ng μl^{-1}; 0.1×, 3.3 ng μl^{-1}) on ice with or without 0.2% saponin to permeabilize mitochondrial membranes.

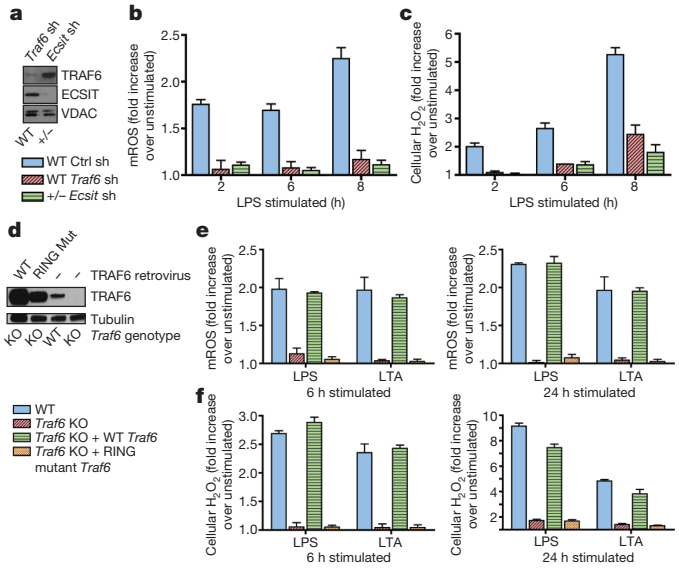

Figure 3 | TRAF6-ECSIT signalling regulates the generation of mitochondrial and cellular ROS, which requires TRAF6 E3-ubiquitin ligase activity. **a**–**c**, Wild-type (WT) or *Ecsit*$^{+/-}$(+/−) BMDMs were transduced with short hairpin RNAs (sh), then either left untreated or stimulated with LPS. **a**, Untreated BMDMs were lysed and extracts blotted for TRAF6 and ECSIT. **b**, **c**, Cells were stained with MitoSOX (**b**) or CM-H_2DCFDA (**c**) and analysed by FACS. **d**–**f**, wild-type or TRAF6-null BMDMs were left alone or transduced with TRAF6-expressing retroviruses, then either left unstimulated or stimulated for the indicated times with LPS or LTA. **d**, Unstimulated BMDMs were lysed and extracts blotted for TRAF6 expression. **e**, **f**, Cells were stained with MitoSOX (**e**) or CM-H_2DCFDA (**f**) and analysed by FACS. All error bars represent s.d. of the mean from triplicate samples.

establish the role of ECSIT in TLR1/2/4-dependent upregulation of mROS, we sought to examine macrophages lacking ECSIT. Although *Ecsit*-knockout mice have been generated, they are very early embryonic lethals[24]. Heterozygous *Ecsit*$^{+/-}$ animals are viable but have ~40% less ECSIT than wild-type animals (Supplementary Fig. 8a). Interestingly, BMDMs from *Ecsit*$^{+/-}$ mice generated modestly lower mROS and cellular H_2O_2 when stimulated with LPS and LTA (Supplementary Fig. 8b, c). To confirm the importance of TLR1/2/4-induced TRAF6–ECSIT signalling in mROS responses, we analysed *Traf6*- and *Ecsit*-knockdown BMDMs (Fig. 3a and Supplementary Fig. 11a). Upon LPS (Fig. 3b) or LTA (Supplementary Fig. 9) stimulation, we observed marked reductions in mROS production in both ECSIT- and TRAF6-depleted macrophages at all time points tested. Although TLR-generated mROS responses were impaired in *Ecsit*-knockdown cells, mROS production elicited by rotenone or antimycin

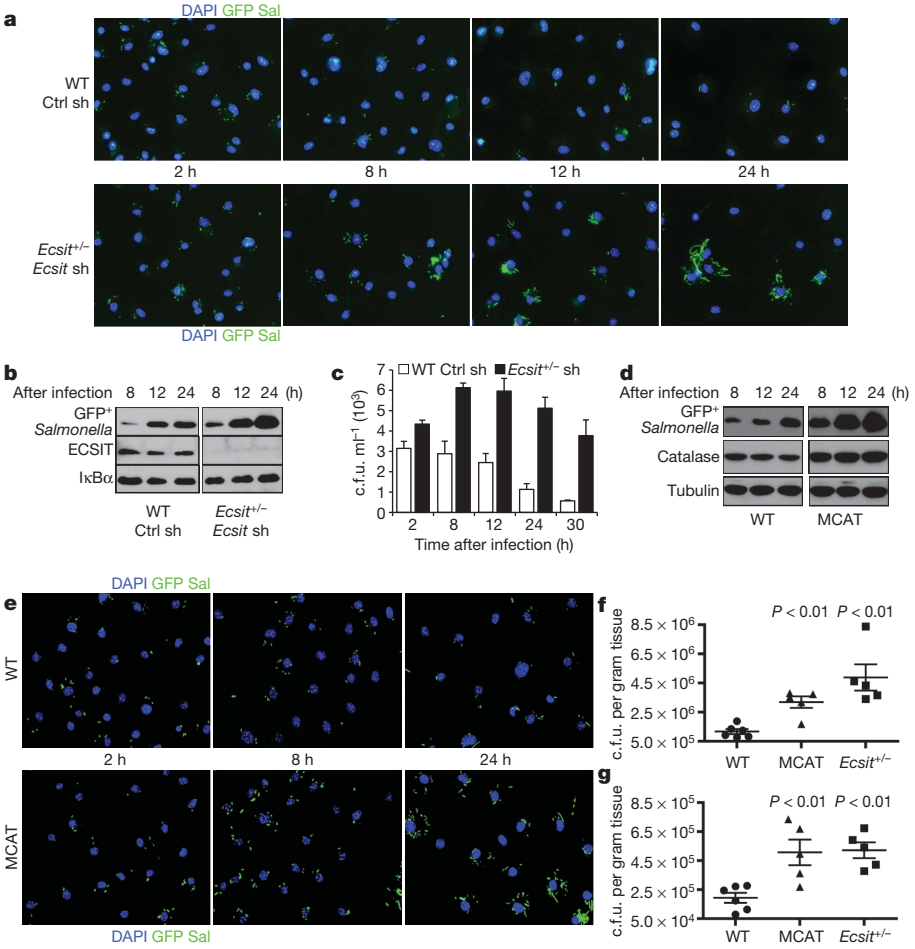

Figure 4 | ECSIT-depleted and MCAT transgenic macrophages are less effective at clearing *Salmonella* than wild-type macrophages. **a**–**c**, BMDMs from wild-type or *Ecsit*$^{+/-}$ mice were transduced with shRNAs and infected with GFP-expressing *Salmonella* (GFP Sal). Cells were fixed and stained with 4′,6-diamidino-2-phenylindole (DAPI) (**a**), solubilized in SDS (**b**) or lysed and plated (**c**). **d**, **e**, wild-type or MCAT BMDMs were infected with GFP-expressing *Salmonella*. Cells were solubilized in SDS (**d**) or fixed and DAPI-stained (**e**). Triplicate wells were pooled and blotted (**b**, **d**), and error bars (**c**) represent s.d. from triplicate samples. **f**, **g**, wild-type ($n = 6$), MCAT ($n = 5$) and *Ecsit*$^{+/-}$ ($n = 5$) mice were infected with *Salmonella* intraperitoneally. Five days after infection, spleens (**f**) and livers (**g**) were homogenized and colony-forming units (c.f.u.) per gram of tissue were determined. Error bars indicate s.e.m. and *P* values are relative to wild-type.

A was unaffected (Supplementary Fig. 10). In addition, LPS- (Fig. 3c and Supplementary Fig. 11b), LTA- (Supplementary Fig. 9) and Pam3CSK4-induced (Supplementary Fig. 11c) cellular H_2O_2 levels were markedly reduced upon *Ecsit* and *Traf6* knockdown. Thus, induction of mROS and cellular H_2O_2 by bacterial PAMPs is critically dependent on both TRAF6 and ECSIT. To determine whether the E3-ubiquitin ligase activity of TRAF6 is required for ROS generation, we examined *Traf6*-knockout BMDMs reconstituted with either wild-type or RING (really interesting new gene) finger domain mutant *Traf6* constructs (Fig. 3d)[25]. In agreement with the knockdown results, TRAF6-null BMDMs generated markedly lower levels of mROS and cellular H_2O_2 in response to both LPS and LTA (Fig. 3e, f). Null macrophages reconstituted with wild-type, but not RING mutant, TRAF6 regained the ability to generate ROS in response to TLR2/4 agonists (Fig. 3e, f). Therefore, these data indicate that a functional RING domain is required for TRAF6 signalling to induce ROS generation, probably because TRAF6 mediates ECSIT ubiquitination (Supplementary Fig. 4).

To test the functional significance of these findings, we assessed the responses of ECSIT- and TRAF6-deficient macrophages to *Salmonella typhimurium*, a Gram-negative, facultative intracellular pathogen that is sensitive to ROS-dependent killing[26–28]. Consistent with the results obtained using purified PAMPs, we observed decreased mitochondrial and cellular ROS in *Ecsit*- and *Traf6*-knockdown BMDMs when exposed to *S. typhimurium* (Supplementary Fig. 12). To determine whether mROS are important in macrophage bactericidal responses, control or *Ecsit*-knockdown BMDMs were infected with GFP-expressing *S. typhimurium* and analysed by immunofluorescence microscopy and western blotting. Notably, ECSIT-depleted BMDMs harboured significantly more GFP-expressing *S. typimurium* than control cells (Fig. 4a, b). The direct measurement of intracellular bacterial colony forming units showed that there were significantly more bacteria in ECSIT-deficient cells than in control cells at all time points examined (Fig. 4c). The reduced ability of ECSIT-deficient BMDMs to control intracellular bacteria was not the result of a non specific impairment of NADPH-oxidase activity, as the PMA-stimulated respiratory burst was unaffected in *Ecsit* knockdowns (Supplementary Fig. 13). Additionally, nitric oxide and proinflammatory cytokine production were similar in control and knockdown BMDMs, collectively indicating that ECSIT depletion does not result in systemic innate immune deficiency (Supplementary Fig. 14).

Mitochondria are regarded as a significant source of H_2O_2 in most cell types and peroxisomal catalase converts H_2O_2 into water and oxygen, reducing oxidative damage caused by these ROS[7]. Overexpressing catalase in mitochondria using transgenic approaches (MCAT mice) leads to significantly lower mitochondrial H_2O_2 levels and these transgenic mice show lower levels of age-related oxidative damage and an extended lifespan[29]. Consistent with our finding that mROS contribute to total cellular ROS levels, MCAT BMDMs generated significantly less LPS-induced cellular H_2O_2 than wild-type cells (Supplementary Fig. 15). To test the specific role of H_2O_2 derived from mitochondria in controlling intracellular bacterial replication, wild-type or MCAT BMDMs were challenged with GFP-expressing *S. typhimurium*. Similar to *Ecsit* knockdowns, MCAT BMDMs had significantly higher bacterial loads than wild-type cells between 8 and 24 h after infection (Fig. 4d, e). Finally, to confirm the role of mROS in control of bacterial infection *in vivo*, we challenged wild-type, MCAT and $Ecsit^{+/-}$ mice by intraperitoneal infection with *S. typhimurium* and measured bacterial burdens in the spleen and liver five days after infection. In agreement with data from isolated BMDMs, both MCAT and $Ecsit^{+/-}$ mice harboured roughly twofold to three fold more bacteria per gram of tissue than wild-type littermates, further substantiating the notion that mROS play an integral part in antibacterial innate immunity (Fig. 4f, g).

We have discovered a novel pathway by which macrophages generate ROS in response to bacteria by coupling TLR1/2/4 signalling to mitochondrial complex I via TRAF6 and ECSIT (Supplementary Fig. 1). Our study demonstrates that in addition to NADPH-oxidase-derived ROS, mROS have an important role in macrophage innate immunity. To our knowledge, this is the first evidence of direct communication between TLRs and mitochondria. This study also highlights a remarkable symmetry between mitochondrial antiviral signalling protein (MAVS) and ECSIT in innate immune responses. As the clearance of intracellular bacteria requires ROS, TRAF6-ECSIT signalling is engaged downstream of bacterial PAMP-sensing TLRs for robust ROS production; likewise, MAVS signalling is activated by virus-sensing RIG-I-like (also known as DDX58) receptors to induce type I interferon production and effective antiviral immunity. Our current findings further solidify the emerging idea that mitochondria serve as hubs for innate immune signalling and the generation of effector responses.

METHODS SUMMARY

Animal strains. *Ecsit*-heterozygous and MCAT mice were previously described and maintained on a C57BL/6 background[24,29].

ROS measurements. Cells were incubated with MitoSOX (to measure the mROS superoxide) and/or CM-H_2DCFDA (to measure total cellular H_2O_2) (Invitrogen) at 2.5 μM final concentration. Unstained controls were treated similarly, except that treatments and dyes were omitted.

Cellular fractionation and mitochondrial isolation. Cell pellets were swelled on ice for 10 min, homogenized with a motorized Teflon pestle, then 2.5× MS buffer (525 mM mannitol, 175 mM sucrose, 12.5 mM Tris-HCl, pH 7.5, 12.5 mM EDTA) was added to 1× final buffer concentration. The homogenate was centrifuged three times at 980*g* for 10 min to pellet nuclei. The supernatant was transferred to a fresh tube and spun at 17,000*g* for 30 min to pellet mitochondria and the resulting cytosolic supernatant was saved for further analysis. The mitochondrial pellet was washed three times with 1× MS buffer, re-suspended in Sucrose-TE (20% sucrose, 50 mM Tris-HCl, pH 7.5, 10 mM EDTA) and then purified additionally by centrifugation through a 1.0–1.5 M sucrose step gradient at 100,000*g* for 60 min. Highly purified heavy mitochondria were removed from the interface of the two sucrose solutions by pipetting and transferred to a fresh tube. Mitochondria were then washed three times with 1 ml of 1× MS buffer and pelleted by centrifugation at 13,000 r.p.m. for 10 min.

Bacterial challenge. Gentamicin protection assays were performed using *S. typhimurium* SL1344 transformed with a GFP expression plasmid essentially as described[30]. *In vivo* challenges were performed by intraperitoneally injecting *S. typhimurium* SL1344 bacteria in 100 μl PBS. Five days after infection, mice were killed, livers and spleens were isolated and tissues were weighed and homogenized in PBS.

Full Methods and any associated references are available in the online version of the paper at www.nature.com/nature.

Received 8 September 2010; accepted 24 February 2011.

1. Lambeth, J. D. NOX enzymes and the biology of reactive oxygen. *Nature Rev. Immunol.* **4,** 181–189 (2004).
2. Arsenijevic, D. *et al.* Disruption of the uncoupling protein-2 gene in mice reveals a role in immunity and reactive oxygen species production. *Nature Genet.* **26,** 435–439 (2000).
3. Rousset, S. *et al.* The uncoupling protein 2 modulates the cytokine balance in innate immunity. *Cytokine* **35,** 135–142 (2006).
4. Sonoda, J. *et al.* Nuclear receptor ERRα and coactivator PGC-1β are effectors of IFN-γ-induced host defense. *Genes Dev.* **21,** 1909–1920 (2007).
5. Vogel, R. O. *et al.* Cytosolic signaling protein Ecsit also localizes to mitochondria where it interacts with chaperone NDUFAF1 and functions in complex I assembly. *Genes Dev.* **21,** 615–624 (2007).
6. Underhill, D. M. & Ozinsky, A. Phagocytosis of microbes: complexity in action. *Annu. Rev. Immunol.* **20,** 825–852 (2002).
7. Koopman, W. *et al.* Mammalian mitochondrial complex I: Biogenesis, regulation and reactive oxygen species generation. *Antioxid. Redox Signal.* 10.1089/ars.2009.2743 (2009).
8. Murphy, M. P. How mitochondria produce reactive oxygen species. *Biochem. J.* **417,** 1–13 (2009).
9. Arnoult, D., Carneiro, L., Tattoli, I. & Girardin, S. E. The role of mitochondria in cellular defense against microbial infection. *Semin. Immunol.* **21,** 223–232 (2009).
10. Adachi, Y. *et al.* IFN-γ primes RAW264 macrophages and human monocytes for enhanced oxidant production in response to CpG DNA via metabolic signaling: roles of TLR9 and myeloperoxidase trafficking. *J. Immunol.* **176,** 5033–5040 (2006).

11. Remer, K. A., Reimer, T., Brcic, M. & Jungi, T. W. Evidence for involvement of peptidoglycan in the triggering of an oxidative burst by *Listeria monocytogenes* in phagocytes. *Clin. Exp. Immunol.* **140,** 73–80 (2005).
12. Werling, D., Hope, J. C., Howard, C. J. & Jungi, T. W. Differential production of cytokines, reactive oxygen and nitrogen by bovine macrophages and dendritic cells stimulated with Toll-like receptor agonists. *Immunology* **111,** 41–52 (2004).
13. West, A. P., Koblansky, A. A. & Ghosh, S. Recognition and signaling by toll-like receptors. *Annu. Rev. Cell Dev. Biol.* **22,** 409–437 (2006).
14. Chong, A., Lima, C. A., Allan, D. S., Nasrallah, G. K. & Garduño, R. A. The purified and recombinant *Legionella pneumophila* chaperonin alters mitochondrial trafficking and microfilament organization. *Infect. Immun.* **77,** 4724–4739 (2009).
15. Horwitz, M. A. Formation of a novel phagosome by the Legionnaires' disease bacterium (*Legionella pneumophila*) in human monocytes. *J. Exp. Med.* **158,** 1319–1331 (1983).
16. Matsumoto, A., Bessho, H., Uehira, K. & Suda, T. Morphological studies of the association of mitochondria with chlamydial inclusions and the fusion of chlamydial inclusions. *J. Electron Microsc. (Tokyo)* **40,** 356–363 (1991).
17. Sinai, A. P., Webster, P. & Joiner, K. A. Association of host cell endoplasmic reticulum and mitochondria with the *Toxoplasma gondii* parasitophorous vacuole membrane: a high affinity interaction. *J. Cell Sci.* **110,** 2117–2128 (1997).
18. Blander, J. M. & Medzhitov, R. Regulation of phagosome maturation by signals from toll-like receptors. *Science* **304,** 1014–1018 (2004).
19. Blander, J. M. & Medzhitov, R. On regulation of phagosome maturation and antigen presentation. *Nature Immunol.* **7,** 1029–1035 (2006).
20. Calvo, S. *et al.* Systematic identification of human mitochondrial disease genes through integrative genomics. *Nature Genet.* **38,** 576–582 (2006).
21. Kopp, E. *et al.* ECSIT is an evolutionarily conserved intermediate in the Toll/IL-1 signal transduction pathway. *Genes Dev.* **13,** 2059–2071 (1999).
22. Chen, Z. J. & Sun, L. J. Nonproteolytic functions of ubiquitin in cell signaling. *Mol. Cell* **33,** 275–286 (2009).
23. Bhoj, V. G. & Chen, Z. J. Ubiquitylation in innate and adaptive immunity. *Nature* **458,** 430–437 (2009).
24. Xiao, C. *et al.* Ecsit is required for Bmp signaling and mesoderm formation during mouse embryogenesis. *Genes Dev.* **17,** 2933–2949 (2003).
25. Deng, L. *et al.* Activation of the IkappaB kinase complex by TRAF6 requires a dimeric ubiquitin-conjugating enzyme complex and a unique polyubiquitin chain. *Cell* **103,** 351–361 (2000).
26. Shiloh, M. U. *et al.* Phenotype of mice and macrophages deficient in both phagocyte oxidase and inducible nitric oxide synthase. *Immunity* **10,** 29–38 (1999).
27. Vazquez-Torres, A. & Fang, F. C. Oxygen-dependent anti-*Salmonella* activity of macrophages. *Trends Microbiol.* **9,** 29–33 (2001).
28. Vazquez-Torres, A. & Fang, F. C. *Salmonella* evasion of the NADPH phagocyte oxidase. *Microbes Infect.* **3,** 1313–1320 (2001).
29. Schriner, S. E. *et al.* Extension of murine life span by overexpression of catalase targeted to mitochondria. *Science* **308,** 1909–1911 (2005).
30. Brodsky, I. E., Ghori, N., Falkow, S. & Monack, D. Mig-14 is an inner membrane-associated protein that promotes Salmonella typhimurium resistance to CRAMP, survival within activated macrophages and persistent infection. *Mol. Microbiol.* **55,** 954–972 (2005).

Supplementary Information is linked to the online version of the paper at www.nature.com/nature.

Acknowledgements We would like to thank C. Schindler, B. Reizis and L. Ciaccia for comments on the manuscript. We also thank P. Rabinovitch for MCAT mice, J. Cotney for technical assistance, Z. Zhang for animal maintenance and M. Graham and K. Zichichi for assistance with immuno-electron microscopy. This work was supported by NIH grants to S.G. (R37-AI33443) and G.S.S. (NS-056206).

Author Contributions A.P.W. designed and performed experiments and wrote the paper; I.E.B. generated GFP-expressing *Salmonella*, helped to design and perform bacterial challenge experiments and edited the paper; C.R. assisted with immuno-electron microscopy; D.K.W. provided MCAT tissues for generating BMDMs; H.E.B. and P.T. performed mass spectrometry analysis; M.C.W. and Y.C. provided reagents and technical advice for experiments involving *Traf6*-knockout cells; G.S.S. designed experiments and edited the paper; S.G. designed experiments and wrote the paper.

Author Information Reprints and permissions information is available at www.nature.com/reprints. The authors declare no competing financial interests. Readers are welcome to comment on the online version of this article at www.nature.com/nature. Correspondence and requests for materials should be addressed to S.G. (sg2715@columbia.edu).

METHODS

Animal strains. *Ecsit* heterozygous and MCAT mice were previously described and maintained on a C57BL/6 background[24,29].

Cell lines and reagents. RAW 264.7, J774A.1 and NOR10 cells were obtained from the ATCC and maintained in DMEM (Invitrogen) containing 5% fetal bovine serum (FBS) (Atlanta Biological). *Escherichia coli* LPS (L6529) and all other chemicals were obtained from Sigma unless otherwise noted. TNF-α was from R&D Systems. CpG 1826 oligonucleotides were synthesized by IDT. *Staphylococcus aureus* LTA, R848 and Pam3CSK4 were purchased from Invivogen. Rabbit polyclonal antibodies against ECSIT were previously described[24]. The following antibodies were also used: mouse monoclonal NDUFS3, VDAC, GRIM19, cytochrome *c* (Mitosciences); goat polyclonal HSP60 and HSP70, rabbit polyclonal IRAK1 and IκBα, mouse monoclonal ubiquitin (Santa Cruz Biotechnology); mouse monoclonal COX1 (Molecular Probes); mouse monoclonal catalase, β-tubulin, Flag M2, HA (Sigma); rabbit monoclonal TRAF6 (Abcam); rabbit polyclonal MAVS and TAK1 (Cell Signaling Technology); mouse monoclonal Dab2 and GFP (BD Biosciences).

ROS measurements. Cells (RAW or BMDMS) were plated in non-tissue-culture-treated six-well dishes and treated with various agonists or stimulated with TLR ligands as indicated. Concentrations of stimulants were as follows: 500 ng ml^{-1} LPS, 1 μg ml^{-1} Pam3CSK4, 2 μg ml^{-1} LTA, 10 μg ml^{-1} poly(I:C), 1 μM CpG, 1 μg ml^{-1} R848, 10 ng ml^{-1} TNF-α, 500 nM rotenone, or 5 μM antimycin A. Culture medium was removed, cells were washed with PBS, then incubated with MitoSOX (to measure the mROS superoxide) and/or CM-H_2DCFDA (to measure total cellular H_2O_2) (Invitrogen) at 2.5 μM final concentration in serum-free DMEM (Invitrogen) for 15 to 30 min at 37 °C. Cells were washed with warmed PBS (37 °C), removed from plates with cold PBS containing 1 mM EDTA by pipetting, pelleted at 1,500 r.p.m. for 3 min, immediately re-suspended in cold PBS containing 1% FBS and subjected to fluorescence-activated cell sorting (FACS) analysis. Unstained controls were treated similarly, except that treatments and dyes were omitted. To control for baseline dye fluorescence, samples from each experiment were left unstimulated but stained according to the above procedure. FACS mean fluorescence intensity values (Figs 3b, c, e, f and Supplementary Figs 11b, c and Fig. 15) were calculated by dividing TLR-stimulated by unstimulated values. Error bars were generated by calculating standard deviation (s.d.) of the mean from triplicate samples. All ROS experiments shown are representative of three independent experiments.

Latex bead phagocytosis assays. Yellow orange 3 micron Fluoresbrite carboxy latex microparticles (Polysciences) were left untreated or coated with 30 μg ml^{-1} LPS or Pam3CSK4 overnight at 4 °C in PBS. Beads were washed ten times in large volumes of PBS containing 1% FBS to remove unbound TLR agonists. BMDMs were cultured on coverslips in 12-well dishes and incubated on ice for 10 min. Microparticles were added at a concentration of approximately 4–8 beads per cell and allowed to settle on the cells for an additional 10 min on ice. Warm medium was added to the cells and plates were moved to 37 °C to allow bead phagocytosis for the indicated times. Cells were then fixed for 20 min at room temperature with paraformaldehyde, permeabilized with 0.1% Triton X-100 and stained with the indicated primary and appropriately labelled secondary antibodies for confocal microscopy. Co-localization and quantification analysis was performed using ImageJ software. Three large fields of view were collected for each condition (each field of view contained roughly 30 cells and approximately 120 yellow orange beads) and the integrated density of the colocalized beads (red pixels) and mitochondria (green pixels) was determined for each image. This value was divided by the total number of beads in each field to determine colocalized pixels per bead and the mean and s.d. were calculated by averaging the three fields of view for each condition. The percentage of beads with mitochondrial cupping (defined as colocalized mitochondria surrounding ~20% or more of the bead periphery) was determined by analysing the same fields of view described above and calculating the mean and s.d. of the percentage values obtained.

Cellular fractionation and mitochondrial isolation. PBS-washed cell pellets were re-suspended in ten pellet volumes of RSB buffer (10 mM NaCl, 1.5 mM $CaCl_2$, 10 mM Tris-HCl, pH 7.5), swelled on ice for 10 min, homogenized with a motorized Teflon pestle, then 2.5× MS buffer (525 mM mannitol, 175 mM sucrose, 12.5 mM Tris-HCl, pH 7.5, 12.5 mM EDTA) was added to 1× final buffer concentration. The homogenate was centrifuged three times at 980*g* for 10 min to pellet nuclei, which were saved for western blot analysis. The supernatant was transferred to a fresh tube and spun at 17,000*g* for 30 min to pellet mitochondria and the resulting cytosolic supernatant was saved for further analysis. The mitochondrial pellet was washed three times with 1× MS buffer, re-suspended in Sucrose-TE (20% sucrose, 50 mM Tris-HCl, pH 7.5, 10 mM EDTA), then purified additionally by centrifugation through a 1.0–1.5 M sucrose step gradient at 100,000*g* for 60 min. Highly purified heavy mitochondria were removed from the interface of the two sucrose solutions by pipetting and were then transferred to a fresh tube. Mitochondria were washed three times with 1 ml of 1× MS buffer and pelleted by centrifugation at 13,000 r.p.m. for 10 min. SDS was then added to nuclear and cytosolic fractions to a final concentration of 1% and mitochondrial pellets were re-suspended in SDS lysis buffer (20 mM Tris-HCl, 1% SDS, pH 7.5) and boiled for 5 min before normalizing protein concentration and western blotting. Fraction purity was confirmed by blotting for IκBα and tubulin (cytoplasm, cyto.), Dab2 (plasma membrane and endosomes, p.m./endos.), and GRIM19 and VDAC (mitochondria, mito.).

Mitochondrial sub-fractionation and Triton X-100 extraction. RAW cell mitochondria were highly purified as above and sub-fractionated as described[31]. For Triton X-100 solubility assay, equal amounts of RAW mitochondria were re-suspended in 1× MS buffer containing the indicated concentrations of Triton X-100 on ice for 20 min. The samples were then spun at 8,000*g* to separate unsolubilized mitochondria from extracted proteins in the supernatant and the resulting pellets were completely solubilized in 1% Triton X-100. Triton concentrations between 0.01% and 0.05% solubilize outer mitochondrial membrane and intermembrane space proteins, whereas concentrations above 0.1% solubilize both outer and inner membrane proteins. Samples were then blotted accordingly.

TRAF6 recruitment and protease sensitivity assays. For the TRAF6 recruitment assay, RAW cells were left untreated or stimulated with TLR agonists (1 μg ml^{-1} LPS, 1 μg ml^{-1} Pam3CSK4, 2 μg ml^{-1} LTA, 1 μM CpG, or 10 μg ml^{-1} poly(I:C)), subjected to mitochondrial isolation as above and fractions were blotted as indicated. For mito-immunoprecipitation, mitochondria were lysed in TNT buffer (25 mM Tris-HCl, pH 7.4, 150 mM NaCl, 1% Triton X-100, 10% glycerol, 1 mM EDTA, protease/phosphatase inhibitors) and incubated with ECSIT antibody and anti-rabbit IgG agarose overnight at 4 °C. The samples were washed extensively and blotted. For the proteinase K sensitivity assay, RAW cells treated with a control shRNA to GFP or with *Traf6* shRNA were left untreated or stimulated with LPS, subjected to mitochondrial fractionation, then purified mitochondria were re-suspended in digest buffer (25 mM Tris-HCl, pH 7.5, 125 mM sucrose, 1 mM $CaCl_2$). Samples were incubated with proteinase K (1×, 33 ng μl^{-1}; 0.1×, 3.3 ng μl^{-1}; ++, 12 ng μl^{-1}; +, 6 ng μl^{-1}) with or without 0.1% saponin on ice for 30 min. Saponin was used to permeabilize mitochondrial membranes gently and allow proteinase K to enter mitochondria. Proteinase K activity was quenched with phenylmethylsulphonyl fluoride (PMSF), SDS was added to 1% to solubilize mitochondrial proteins and samples were blotted as indicated.

Ubiquitination assays. For endogenous ubiquitination assays, one 10-cm dish of J774 control *GFP* shRNA or *Traf6* shRNA cells per time point was stimulated as described and solubilized in boiling SDS lysis buffer, then boiled for an additional 10 min. After shearing DNA, the samples were diluted in 2× TNT buffer to 1× and immunoprecipitated overnight with ECSIT antibody and anti-rabbit IgG beads (eBioscience). Beads were washed in 1× TNT buffer and samples were blotted and probed with antibodies as indicated. All other ubiquitination assays were performed using 6-cm dishes of 293T cells transfected with 0.25–1 μg each of the indicated constructs. After overnight incubation (and 2 h incubation in MG132, if indicated), cells were lysed as described above, diluted in 2× TNT buffer and immunoprecipitated with anti-Flag resin (Sigma) overnight. Beads were washed extensively and samples blotted and probed as indicated. TRAF6, ECSIT-FLAG, and ΔN-ECSIT–Flag were previously described[21].

Bacterial infection and gentamicin protection assay. Gentamicin protection assays were performed using *S. typhimurium* SL1344[32] transformed with a GFP expression plasmid essentially as described[30,33]. Briefly, BMDMs were plated at 2×10^5 cells per well in 24-well dishes, incubated with opsonized (using fresh mouse serum) GFP-expressing *Salmonella* at a multiplicity of infection of 20 for 1 h, then further incubated with 100 μg ml^{-1} gentamicin for 1 h. Wells were washed several times and 2 h time points were collected or cells further incubated in media containing 10 μg ml^{-1} gentamicin. Similar results were obtained when the initial 100 μg ml^{-1} gentamicin incubation was omitted and cells were only exposed to 10 μg ml^{-1} gentamicin (not shown). For colony count analysis, triplicate samples were lysed in PBS containing 1% Triton X-100, serially diluted in PBS and plated on LB agar plates containing streptomycin. For western blot analysis of GFP-expressing *Salmonella*, triplicate BMDMs samples were infected as above and cells were lysed at indicated time points in SDS lysis buffer. After boiling and shearing DNA, samples were pooled and blotted as described. For immunofluorescence analysis of GFP-expressing *Salmonella*, 2×10^5 BMDMs were grown on coverslips in 12-well dishes and treated as above. At indicated time points, cells were fixed with 4% paraformaldehyde for 20 min at room temperature, nuclei stained with DAPI and cells mounted and imaged by confocal microscopy. Experiments shown are representative of at least three independent experiments.

***In vivo Salmonella* infection assay.** 8–10-week-old wild-type, MCAT, or *Ecsit*$^{+/-}$ littermates were injected intraperitoneally with 200 *S. typhimurium* SL1344 bacteria in 100 μl PBS. Five days after infection, mice were killed, livers and spleens were isolated and tissues were weighed and homogenized in 1 ml PBS.

Lysates were serially diluted in PBS and 100 µl of each dilution was plated on LB streptomycin plates. Colonies were counted the next morning with a BioRad VersaDoc imager using the colony counting feature of the Quantity One software. Error bars represent standard error of the mean (s.e.m.).

Tandem affinity purification and mass spectrometry. 293T or RAW cells were transiently or stably transfected with pCTAP-ECSIT (primers used: F, tacgagtcc gaattcccaccatgagctgggtgcaggtcaac; R, tacgagtccctcgagactttgcccctgctgctgctc) respectively and TAP complexes were purified using the Interplay Mammalian TAP System (Stratagene) as described. Purified complexes were precipitated in 10% trichloroacetic acid, washed with cold acetone, air dried and re-suspended in 4× Laemmli sample buffer. Samples were electrophoresed on SDS–polyacrylamide gel electrophoresis (SDS–PAGE) gels until just entering the resolving gel, slices were removed and subjected to in-gel trypsin digestion and mass spectrometry analysis in the laboratory of P. Tempst at Memorial Sloan-Kettering Cancer Center as described[34,35].

Immuno-electron microscopy. J774 cells were left untreated or stimulated with LPS, washed with PBS and fixed (2% paraformaldehyde, 0.1% gluteraldehyde, 3% sucrose, 0.25 M HEPES, pH 7.4) for 30 min at 4 °C. Samples were then rinsed in PBS and re-suspended in 10% gelatin, chilled and trimmed to smaller blocks, then placed in cryoprotectant (2.3 M sucrose) rotating overnight at 4 °C. Small pieces were transferred to aluminium pins and frozen rapidly in liquid nitrogen. The frozen block was trimmed on a Leica Cryo-EMUC6 UltraCut and 75-nm-thick sections were collected using the Tokoyasu method (1973), placed on a nickel formvar/carbon-coated grid and floated in a dish of PBS ready for immunolabelling. Grids were placed section-side-down on drops of 0.1 M ammonium chloride for 10 min to quench untreated aldehyde groups, then blocked for nonspecific binding on 1% fish skin gelatin in PBS for 20 min. Single labelled grids were incubated in primary rabbit anti-ECSIT antibody at 1:20 dilution for 30 min. After rinsing, the grids were placed on protein A gold (UtrechtUMC) for 30 min. All grids were rinsed in PBS, fixed with 1% gluteraldehyde for 5 min, rinsed in water and transferred to a 0.5% uranyl acetate/1.8% methylcellulose drop for 10 min, then collected and dried. Grids were viewed with a FEI Tencai Biotwin TEM at 80 KV. Images were taken using a Morada CCD and item software (Olympus).

Bone marrow macrophage generation and lentiviral shRNA/retroviral transduction. Bone marrow was collected from littermate wild-type, *Ecsit*$^{+/-}$ or MCAT mice and cultured on Petri plates for a period of 7 days in DMEM containing 10% FBS plus 30% L929 conditioned media. Media was replenished on day four of culture. Lentiviral shRNA constructs were purchased from Open Biosystems (pLKO.1 vector control ID RHS4080; GFP targeting control clone ID RHS4459; ECSIT clone ID TRCN0000113957 or TRCN0000113958 ; TRAF6 clone ID TRCN0000040733 or TRCN0000040735) and were packaged as described in the Broad Institute RNAi Consortium protocols (http://www.broadinstitute.org/genome_bio/trc/publicProtocols.html) using 239FT cells (Invitrogen). Macrophages were transduced with shRNA lentiviruses overnight on day three of culture and media were changed on day four as above, except that 3 µg ml^{-1} puromycin was added for the remainder of culture to select transduced cells. On day seven, cells were lifted from plates by incubating in cold TEN buffer (40 mM Tris-HCl, pH 7.4, 150 mM NaCl, 1 mM EDTA), re-plated in fresh media without puromycin containing 10% L929 conditioned media and allowed to rest for a period of 24–48 h before experimentation. RAW cells stably expressing control, *GFP*, *Traf6*, or *Ecsit* shRNAs were selected by puromycin resistance and maintained in 3–4 µg ml^{-1} puromycin.

Ecsit knockdown experiments both in the main Figures and in the Supplementary Figures used shRNA clone ID TRCN0000113958 (termed *Ecsit* sh) except Supplementary Fig. 11, which used clone ID TRCN0000113957 (termed *Ecsit* sh4). All *Traf6* knockdown experiments used shRNA clone ID TRCN0000040735 (termed *Traf6* sh) with the exception of Supplementary Fig. 11, which used clone ID TRCN0000040733 (termed *Traf6* sh1). We observed similar knockdowns and deficiencies in both mitochondrial and cellular ROS production compared to control when either *Traf6* or *Ecsit* shRNA clone was used but have not included both data sets because of space limitations. Furthermore, we detected no significant differences in ROS production or bacterial killing between macrophages transduced with vector control or GFP control shRNAs; therefore, most of the control samples were transduced with vector control lentiviruses. Finally, we used wild-type BMDMs for control and *Traf6*-knockdown experiments but *Ecsit*$^{+/-}$ BMDMs for *Ecsit* knockdowns. Heterozygous BMDMs have a ~40% reduction in total ECSIT protein abundance by western blot (Supplementary Fig. 11a); therefore, we used these cells to allow for more robust reduction in ECSIT levels upon shRNA silencing. We used age- and sex-matched littermate controls for the wild-type Ctrl and *Traf6* knockdowns, thus minimizing animal to animal variation when comparing wild-type and +/− samples to one another. TRAF6-null BMDMs generation and retroviral reconstitution with WT and RING mutant constructs was performed as previously described[36].

Confocal microscopy. For all microscopy images, cells were grown on coverslips and transfected, stimulated or infected as described. After washing, cells were fixed with 4% paraformaldehyde for 20 min, permeabilized with 0.1% Triton X-100 in PBS for 5 min, blocked with PBS containing 10% FBS for 30 min, stained with primary antibodies for 6 min, then stained with secondary antibodies for 60 min. Cells were washed with PBS between each step. Nuclei were stained with TOPRO3 (Invitrogen) or DAPI (Sigma) and coverslips were mounted with Prolong Gold anti-fade reagent (Molecular Probes). Cells were imaged on a Zeiss LSM 510 META with a 63× water-corrected objective.

Amplex Red assay. 1×10^5 wild-type or *Ecsit*$^{+/-}$ BMDMs infected with control or *Ecsit* shRNA-expressing lentiviruses were plated in 96-well fluorescence microplates (Costar). After two PBS washes to remove residual medium, cells were re-suspended in 100 µl pre-warmed, sterile Hank's buffered salt solution containing 50 µM Amplex Red (Invitrogen) and 1 U ml^{-1} horseradish peroxidase (Sigma) with or without PMA or serum-opsonized *Salmonella* SL1344 for the indicated times. Oxidation of Amplex Red into red-fluorescent resorufin by H_2O_2 was measured in a fluorescence plate reader using excitation at 530 nm and fluorescence detection at 590 nm. Molar concentrations of extracellular peroxide were determined by comparing fluorescence values from each sample with those generated from a standard curve of H_2O_2. Average background fluorescence readings from unstimulated triplicate wells were subtracted from each sample that was stimulated with PMA or infected with *Salmonella*. This allowed for measurement of the amount of H_2O_2 that was induced over unstimulated samples during the same time interval and normalized for cell plating errors.

Nitric Oxide and ELISA assays. Wild-type or *Ecsit*$^{+/-}$ BMDMs were infected with control, *Traf6* or *Ecsit* shRNA-expressing lentiviruses, plated in 24-well dishes and left untreated or stimulated with 1 µgml^{-1} LPS for the indicated times. Supernatant was collected, serially diluted and measured for nitrite by the Griess Reagent Kit (Molecular Probes) or for TNF-α and IL-12p40 by ELISA (eBioscience) as per the manufacturers' instructions.

31. Kang, B. H. *et al.* Regulation of tumor cell mitochondrial homeostasis by an organelle-specific Hsp90 chaperone network. *Cell* **131,** 257–270 (2007).
32. Hoiseth, S. K. & Stocker, B. A. Aromatic-dependent *Salmonella typhimurium* are non-virulent and effective as live vaccines. *Nature* **291,** 238–239 (1981).
33. Valdivia, R. H. & Falkow, S. Bacterial genetics by flow cytometry: rapid isolation of Salmonella typhimurium acid-inducible promoters by differential fluorescence induction. *Mol. Microbiol.* **22,** 367–378 (1996).
34. Cooper, M. P. *et al.* Defects in energy homeostasis in Leigh syndrome French Canadian variant through PGC-1α/LRP130 complex. *Genes Dev.* **20,** 2996–3009 (2006).
35. Sebastiaan Winkler, G. *et al.* Isolation and mass spectrometry of transcription factor complexes. *Methods* **26,** 260–269 (2002).
36. Walsh, M. C., Kim, G. K., Maurizio, P. L., Molnar, E. E. & Choi, Y. TRAF6 autoubiquitination-independent activation of the NFκB and MAPK pathways in response to IL-1 and RANKL. *PLoS ONE* **3,** e4064 (2008).